Suppl. material for LHCb-PAPER-2017-035

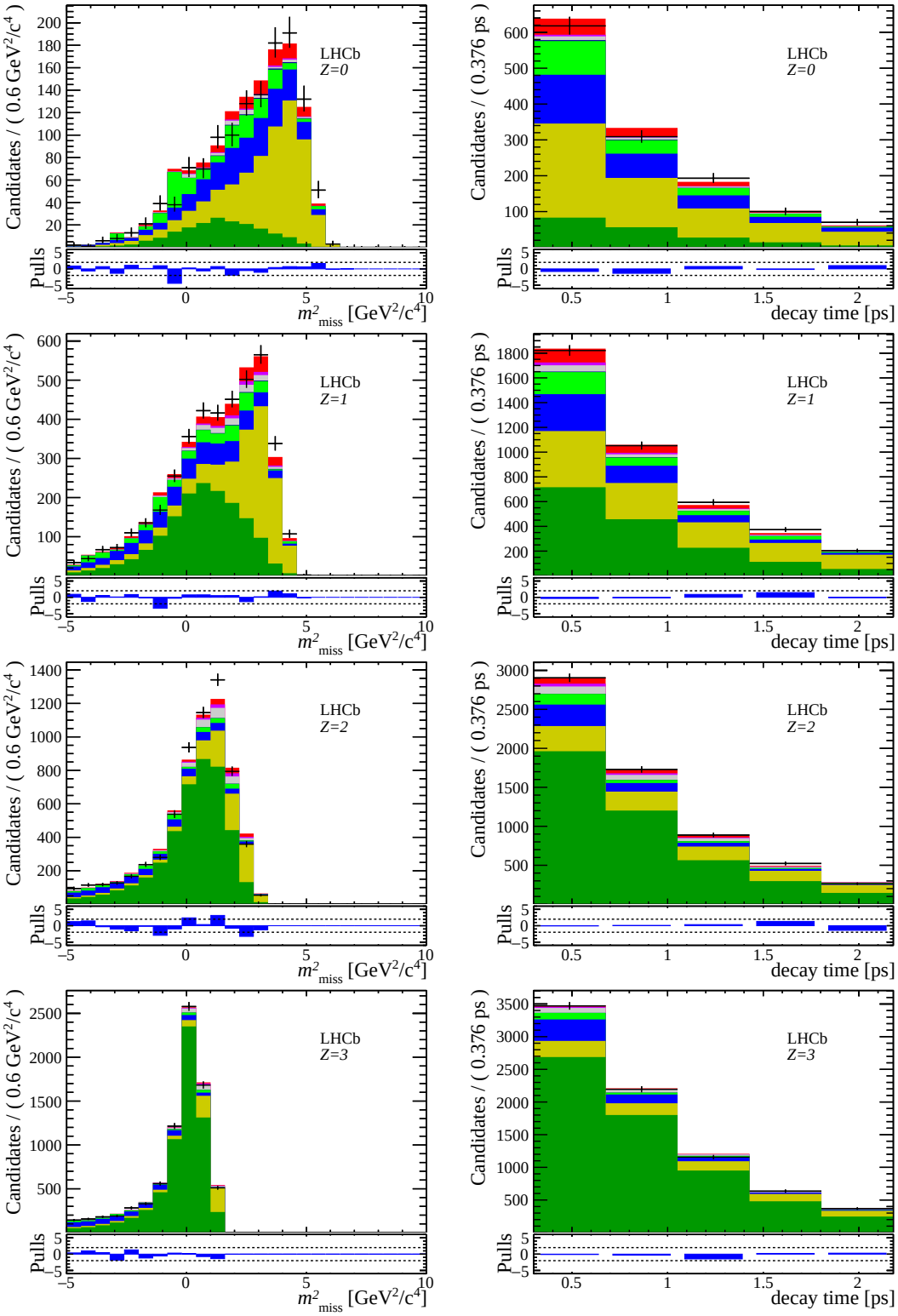

Figure 1: Projections of the nominal fit in bins 0–3 of Z, *i.e.* individual bins of q^2 and E^*_μ.

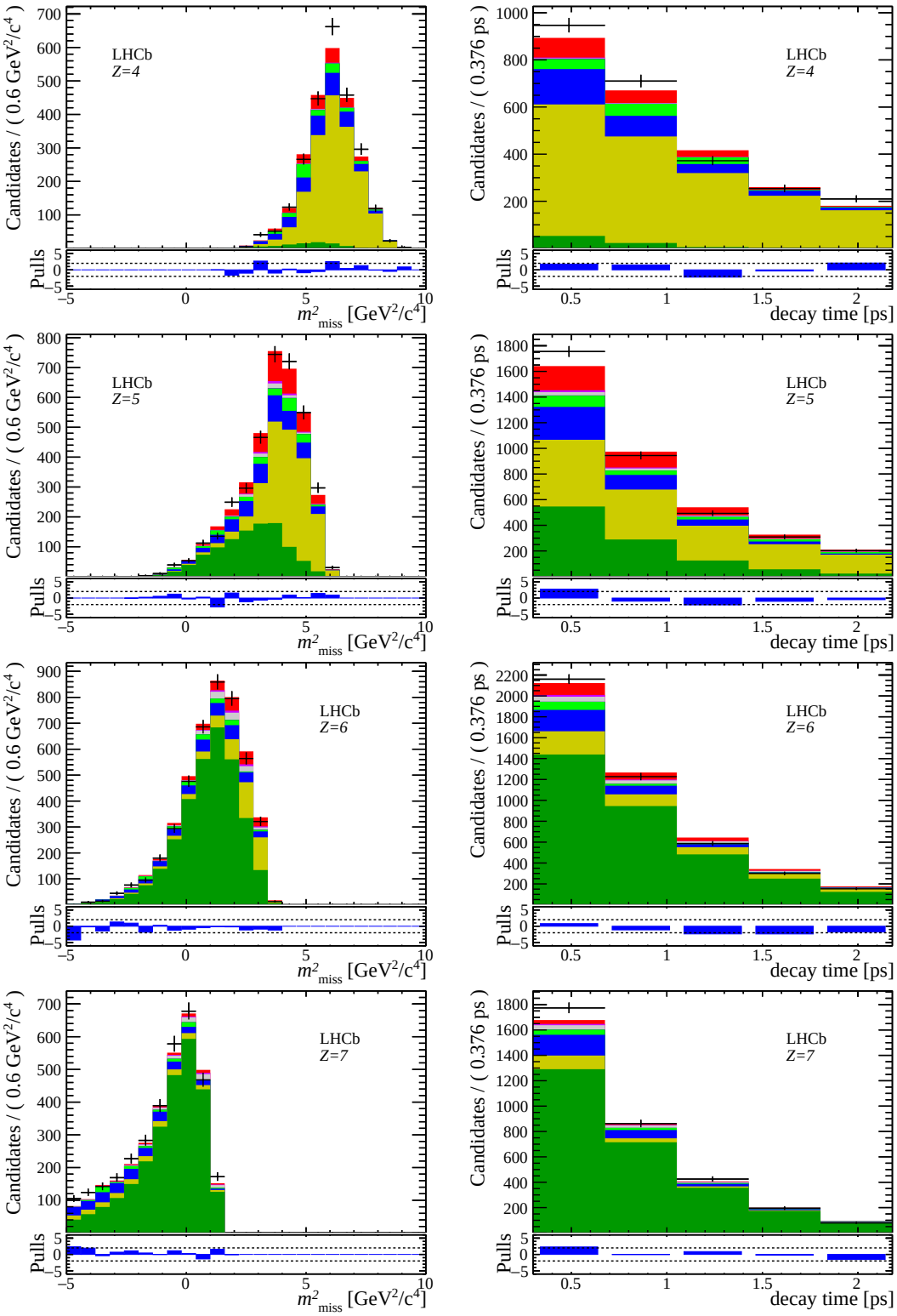

Figure 2: Projections of the nominal fit in bins 4–7 of Z, *i.e.* individual bins of q^2 and E_μ^*.

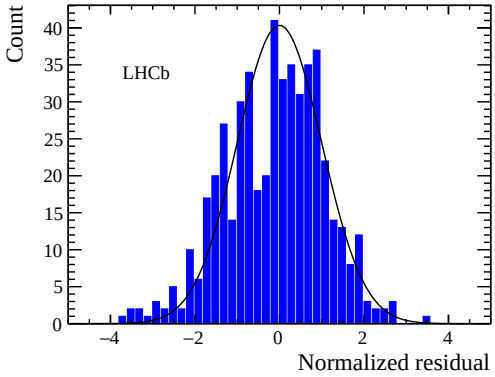

Figure 3: Distribution of normalized residuals of the 1000 bins of the nominal fit. A standard normal distribution is superimposed.

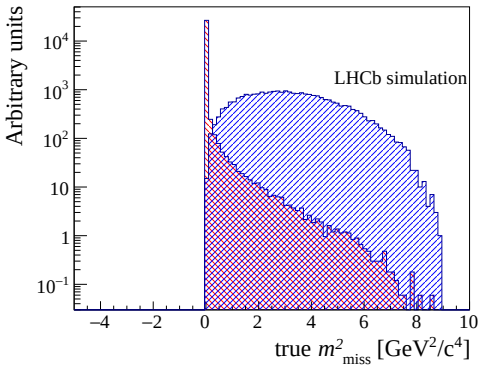

(a) True m^2_{miss} distribution

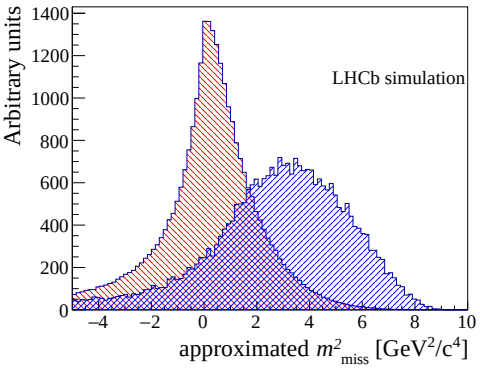

(b) Smeared m^2_{miss} distribution

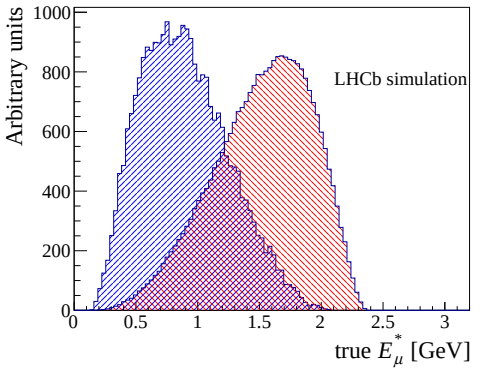

(c) True E^*_μ distribution

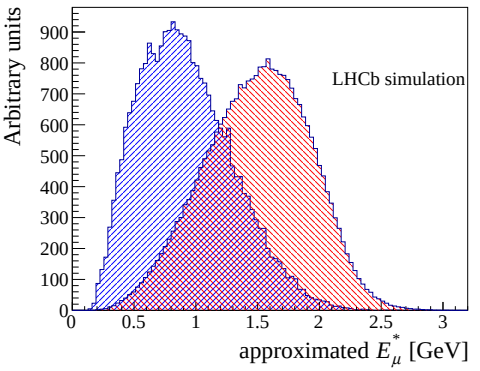

(d) Smeared E^*_μ distribution

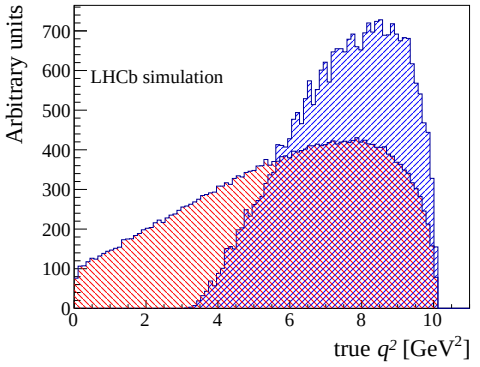

(e) True q^2 distribution

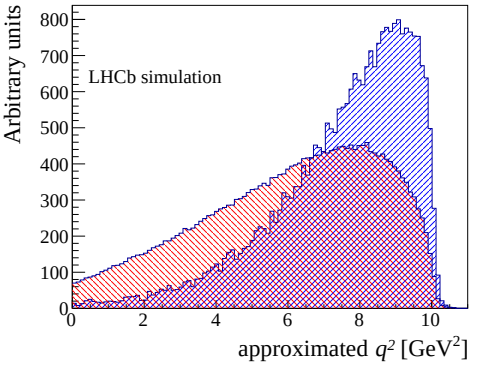

(f) Smeared q^2 distribution

Figure 4: For each fit quantity (save the mostly unaltered decay time), the distributions of the quantity calculated using the simulated true B_c^+ momentum and the approximated momentum are shown. In each plot, the normalization $B_c^+ \to J/\psi\,\mu^+\nu_\mu$ decay is shown in red, while the signal $B_c^+ \to J/\psi\,\tau^+\nu_\tau$ is shown in blue. After the smearing induced by the rest frame approximation, enough discriminating power remains in these quantities to make the measurement feasible.

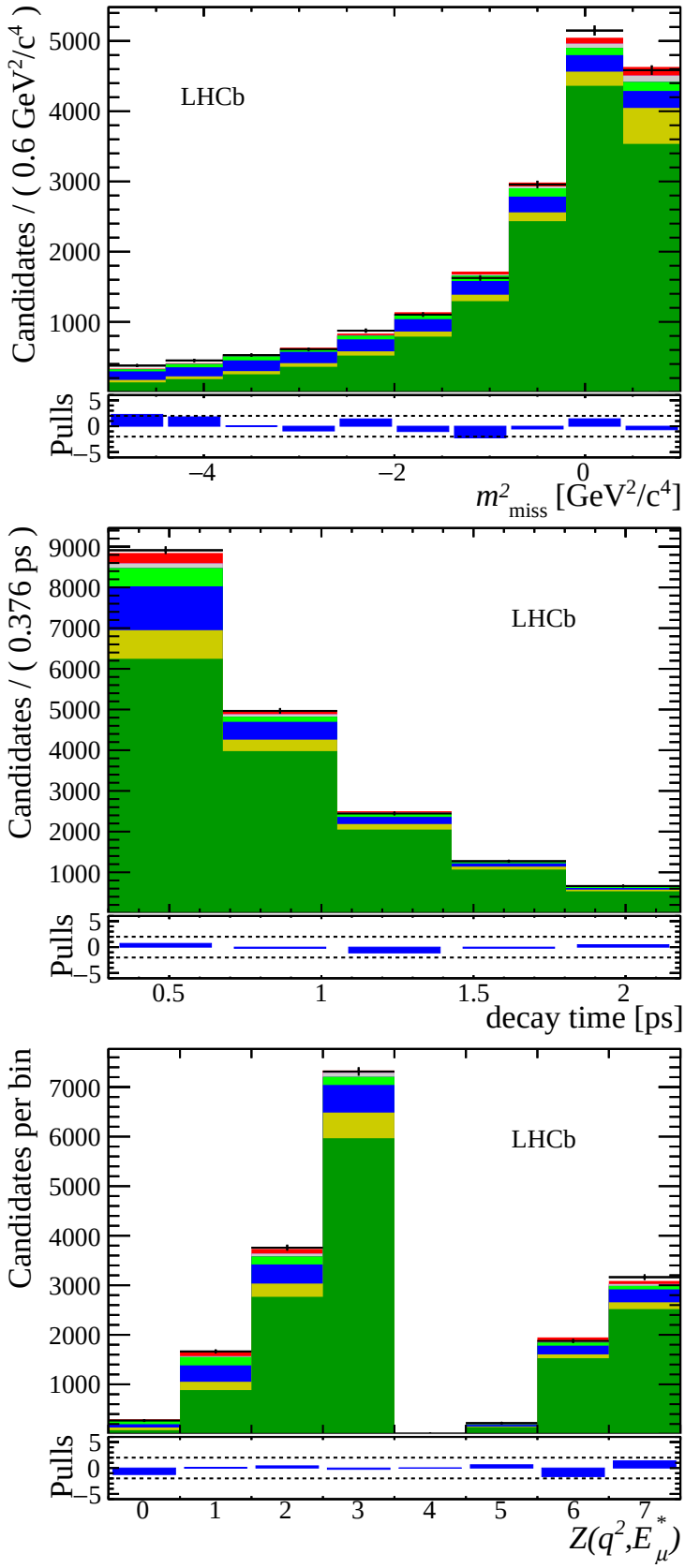

Figure 5: Projections of the fit to a region enriched and relatively pure in $B_c^+ \to J/\psi\,\mu^+\nu_\mu$, by applying tighter isolation criteria and an upper bound of 1 GeV$^2/c^4$ for the missing mass squared, used to determine the non-timelike form factors.

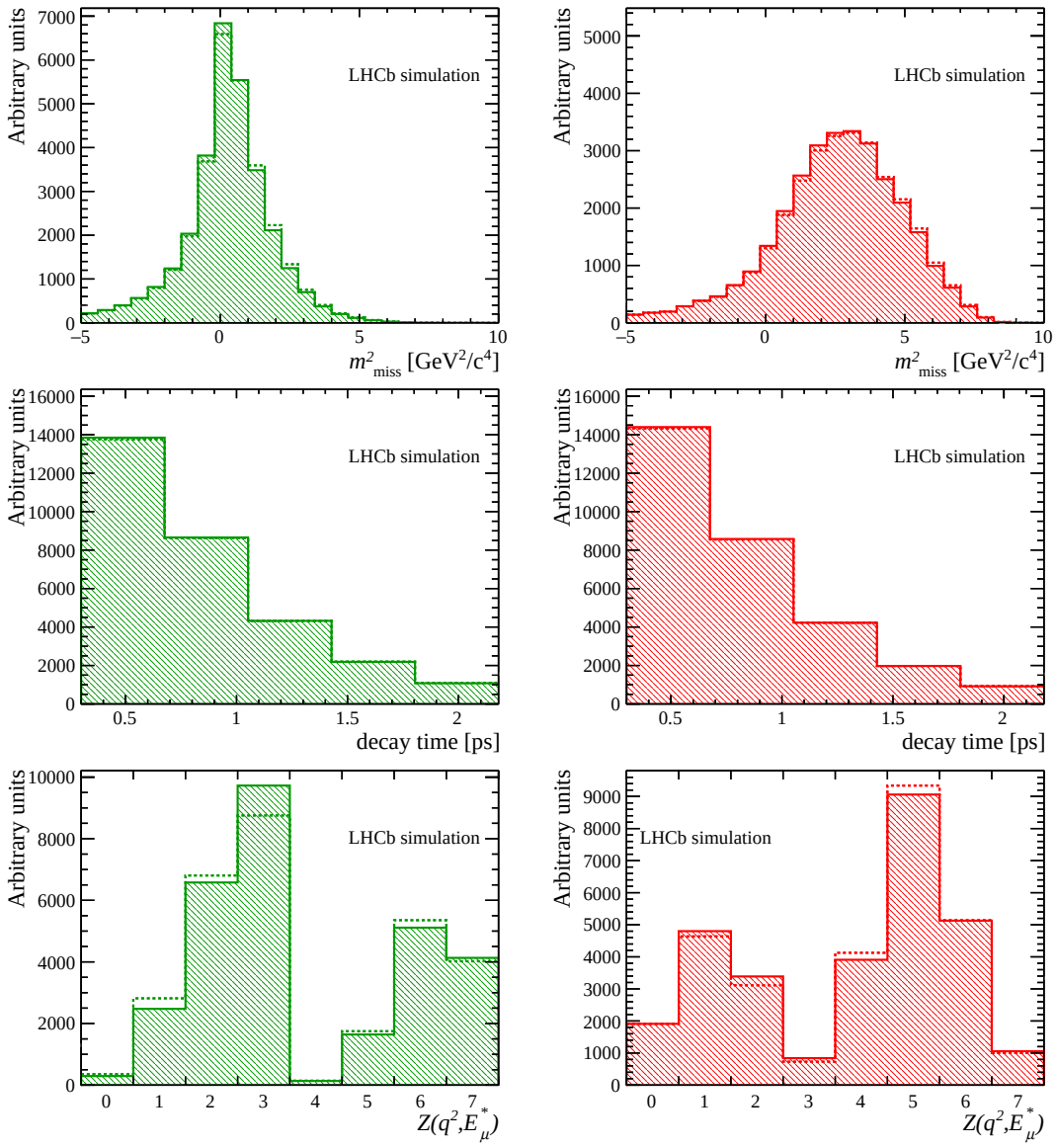

(a) Correction to the normalization distribution

(b) Correction to the signal distribution

Figure 6: Comparisons of the original uncorrected distributions of the normalization and signal using the form factor model of Ref. [**?**] (unfilled dashed histograms, in green and red respectively) with the distributions corrected by the measured form factors (cross-hatched solid histograms, in green and red respectively). The changes are relatively small, but crucially important to the quality of the fit. The yields in these plotted distributions are arbitrary.

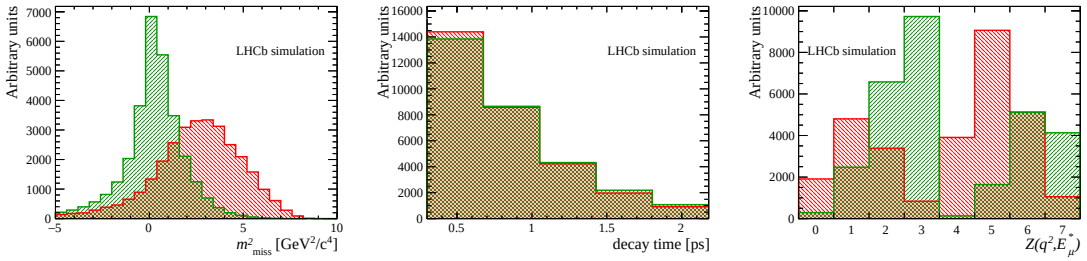

(a) Normalization

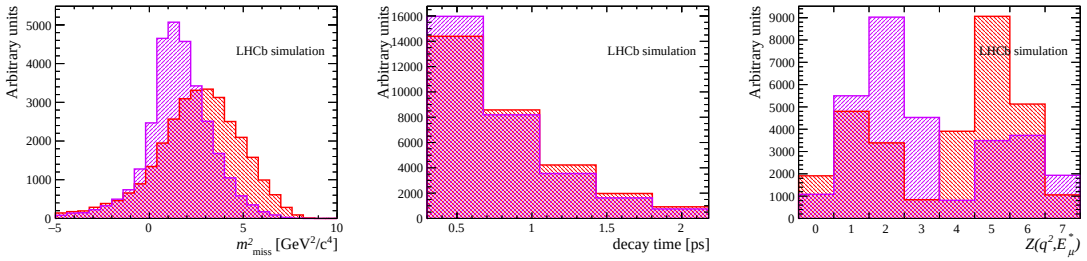

(b) $\psi(2S)$ feed-down

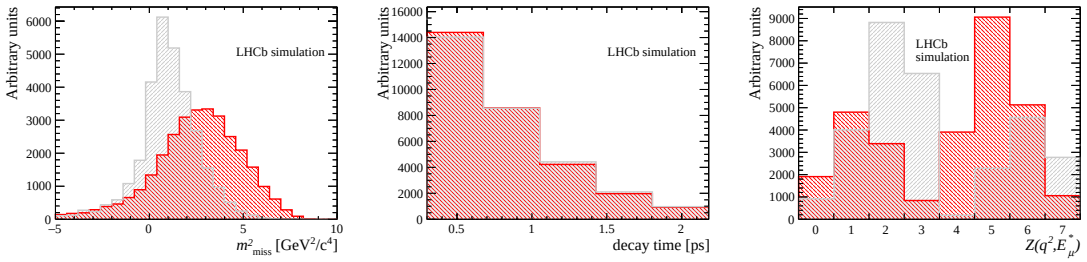

(c) $\chi_c(1P)$ feed-down

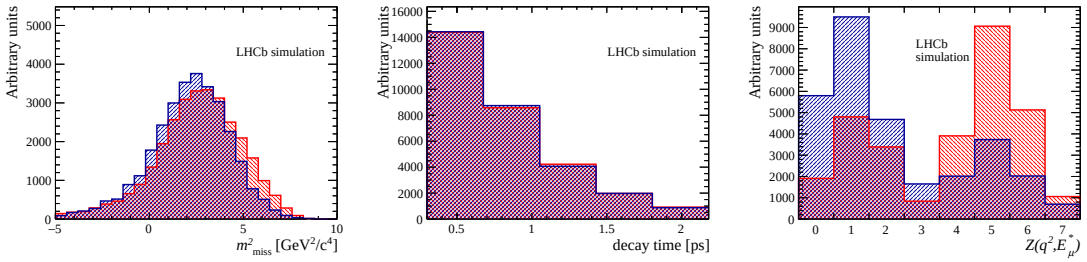

(d) Double-charm background

Figure 7: Comparisons of each set of background distributions (in various colors according to the legend) to the signal distribution (in red). Similar backgrounds, such as the separate $\chi_c(1P)$, combinatorial, or mis-ID modes are grouped together for simplicity. Continued below.

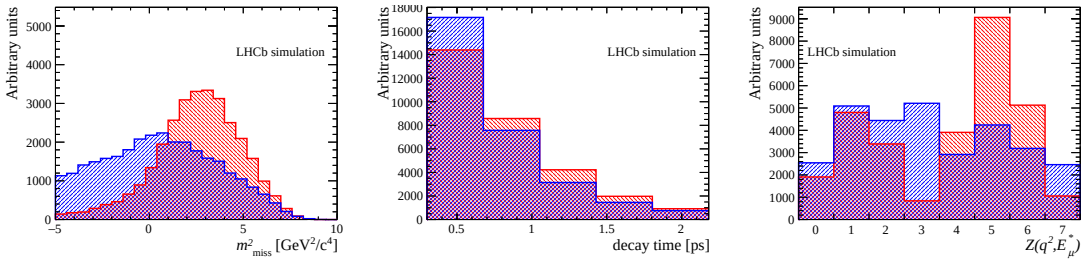

(a) Combinatorial J/ψ background

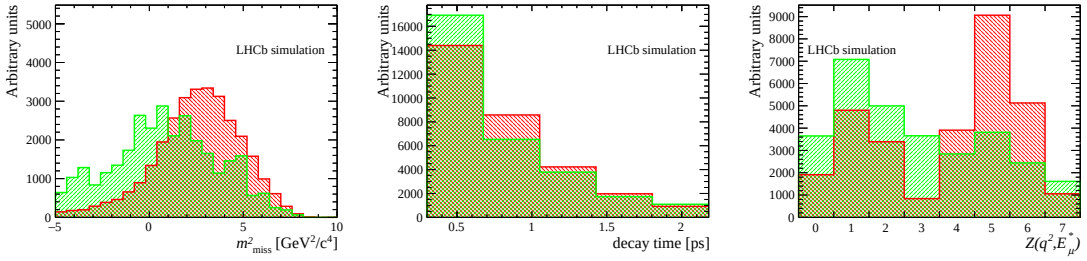

(b) Combinatorial $J/\psi\,\mu$ background

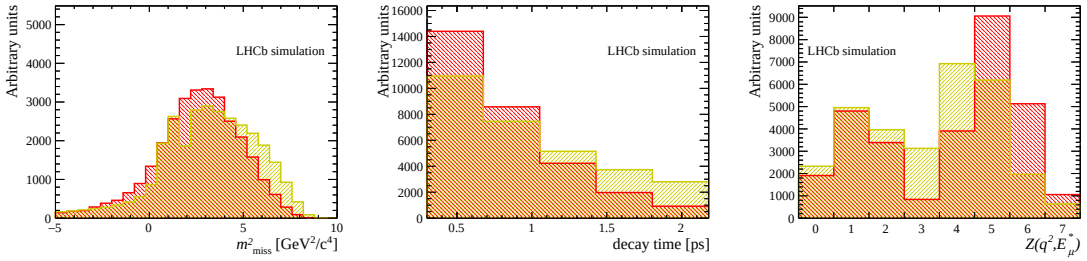

(c) Mis-ID background

Figure 8: Comparisons of each set of background distributions (in various colors according to the legend) to the signal distribution (in red). Similar backgrounds, such as the separate $\chi_c(1P)$, combinatorial, or mis-ID modes are grouped together for simplicity. Continuation of above.

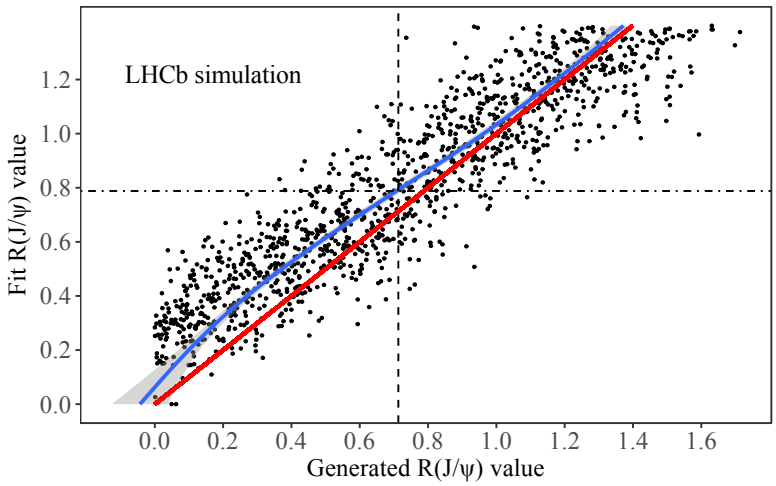

Figure 9: In the pseudoexperiments, both the fit templates and the data are sampled from densities obtained by kernel density estimation (KDE), which essentially interpolates bins that would be otherwise empty in the raw histogram templates. The pairs of generated values of $\mathcal{R}(J/\psi)$ (x-axis), sampled from a uniform distribution, and measured values (y-axis) are shown as black points; both values are corrected for the signal to normalization efficiency ratio. The conditional true value given a fixed measured value — measured by a LOESS curve (a type of local linear regression) plotted by a blue line with a grey error band — is the Bayesian bias correction given a uniform prior. The line $y = x$ is plotted in red for reference.